Journal of the Korean Ceramic Society
Vol. 52, No. 5, pp. 344~349, 2015.

http://dx.doi.org/10.4191/kcers.2015.52.5.344

Lanthanum Nickelates with a Perovskite Structure as Protective Coatings on Metallic Interconnects for Solid Oxide Fuel Cells

Nurhadi S. Waluyo*,, Beom-Kyeong Park*, Rak-Hyun Song*, Seung-Bok Lee*, Tak-Hyoung Lim*, Seok-Joo Park*, and Jong-Won Lee*,**,†**

*New and Renewable Energy Research Division, Korea Institute of Energy Research, Daejeon 34129, Korea
**Department of Advanced Energy and Technology, Korea University of Science and Technology (UST), Daejeon 34113, Korea

(Received July 29, 2015; Revised August 22, 2015; Accepted August 24, 2015)

ABSTRACT

An interconnect is the key component of solid oxide fuel cells that electrically connects unit cells and separates fuel from oxidant in the adjoining cells. To improve their surface stability in high-temperature oxidizing environments, metallic interconnects are usually coated with conductive oxides. In this study, lanthanum nickelates ($LaNiO_3$) with a perovskite structure are synthesized and applied as protective coatings on a metallic interconnect (Crofer 22 APU). The partial substitution of Co, Cu, and Fe for Ni improves electrical conductivity as well as thermal expansion match with the Crofer interconnect. The protective perovskite layers are fabricated on the interconnects by a slurry coating process combined with optimized heat-treatment. The perovskite-coated interconnects show area-specific resistances as low as 16.5 - 37.5 m $\Omega \cdot cm^2$ at 800°C.

Key words : Solid oxide fuel cell, Metallic interconnect, Protective coating, Perovskite oxide, Lanthanum nickelate

1. Introduction

Solid oxide fuel cells (SOFCs) have been considered promising energy conversion systems with potential advantages over low-temperature fuel cells (*e.g.*, polymer electrolyte membrane fuel cells), including fast electrode kinetics, high tolerance to catalyst poisons, and fuel flexibility.[1)] In an SOFC stack, an interconnect electrically connects unit cells and separates fuel from oxidant in the adjoining cells.[2-4)] The key material requirements for SOFC interconnects include the following:[2)] (*i*) high electronic conductivity but negligible ionic conductivity; (*ii*) high chemical/structural stability in a dual atmosphere; (*iii*) high density (low porosity) to ensure separation between fuel and oxidant; (*iv*) coefficients of thermal expansion compatible with those of other SOFC components; and (*v*) low material/fabrication cost. Among various metallic alloys under development, ferritic stainless steels have been the materials of choice for SOFC interconnects.[5)] However, chromia (Cr_2O_3) scales with very low electrical conductivity are known to grow continuously during SOFC operations, leading to a considerable increase of interfacial resistance.[6–9)] In addition, several studies have reported severe degradation of cathodes in the presence of metallic interconnects; this degradation is caused by evaporation of gaseous Cr species from the chromia scales, followed by electrochemical reduction on the active sites of cathodes (*i.e.*, Cr poisoning).[10-12)]

Surface modification of metallic interconnects with conductive oxide coatings is a practical solution to mitigate the problems mentioned above. Some spinel-type metal oxides based on Mn and Co are known to possess the capability to reduce the growth rate of chromia scales and to inhibit Cr migration from the chromia-rich layer toward the cathode at high temperatures.[13,14)] Furthermore, mixed metal oxides with perovskite structure are considered promising coating materials for metallic interconnects because they exhibit high electrical conductivity and good thermal expansion match as well as high chemical/structural stability under typical SOFC operating conditions. To date, much research has focused on lanthanum manganites ($LaMnO_3$) doped with Sr and other elements; these materials have high electronic conductivity but relatively low oxygen permeability.[15-17)] Recently, Choi *et al.*[18)] and Ni *et al.*[19)] investigated perovskite-type lanthanum nickelates ($LaNiO_3$) as protective coatings on metallic interconnects; they demonstrated that $LaNiO_3$-coated interconnects show resistances lower than those of $LaMnO_3$-coated interconnects. In addition to the high intrinsic conductivity of $LaNiO_3$, the interdiffusion reaction between Ni (in $LaNiO_3$) and Mn (in Mn-containing Cr_2O_3) has been proposed to be responsible for the reduced resistivity of interfacial chromia scales.[20)]

In this work, $LaNiO_3$ perovskites, in which different cations were substituted for parts of Ni, were synthesized and applied as protective coatings on metallic interconnects for SOFCs. Nano-sized perovskite oxides were prepared by the Pechini method using citric acid. Structural, electrical, and thermal expansion properties of the synthesized materials were determined using various analytical tools. Perovskite coatings were fabricated on a metallic interconnect (Crofer

†Corresponding author : Jong-Won Lee
E-mail : jjong277@kier.re.kr
Tel : +82-42-860-3025 Fax : +82-42-860-3297

22 APU) using a slurry dip-coating process combined with optimized heat-treatment; then, the area-specific resistances of the coated interconnects were determined in an air atmosphere at various temperatures.

2. Experimental Procedure

2.1. Material synthesis and sintering

The precursors used for the preparation of pure and doped $LaNiO_3$ powders were lanthanum nitrate ($La(NO_3)_3 \cdot 6H_2O$, 99%, Kanto Chemical), nickel nitrate ($Ni(NO_3)_3 \cdot 6H_2O$, 99%, Sigma-Aldrich), cobalt nitrate ($Co(NO_3)_2 \cdot 6H_2O$, 99%, Sigma-Aldrich), copper nitrate ($Cu(NO_3)_2 \cdot 2.5H_2O$, ≥ 98%, Sigma-Aldrich), and iron nitrate ($Fe(NO_3)_3 \cdot 9H_2O$, ≥ 98%, Sigma-Aldrich). The required amounts of the precursors were dissolved in distilled water. Citric acid ($HOC(COOH)(CH_2COOH)_2$, ≥ 99.5%, Junsei Chemical) was added to the mixed solution under magnetic stirring; then, the solution was heated to 90°C. The molar ratios of metal ions and citric acid for pure and doped $LaNiO_3$ materials were maintained at 1 : 5 and 1 : 3, respectively. The resulting solution was heated to 150°C to form a viscous gel. After this, the gel was dried at 250°C and then calcined at 800°C for 5 h to produce perovskite-type oxide powders. For electrical and thermal expansion determination, the Pechini-derived powders were uniaxially pressed into bars under a pressure of 30 MPa. The green body was sintered in air at 1050°C for 5 h.

2.2. Coating of protective layers on a metallic interconnect substrate

Crofer 22 APU (ThyssenKrupp VDM, GmBH, Germany, 1 mm in thickness) was used as a metallic interconnect substrate. The substrate was cut into a coupon with dimensions of 20 mm × 20 mm and was then grinded with 800 grit SiC paper. A slurry was prepared by mixing the perovskite powders with toluene, isopropanol alcohol, and binders; then, the Crofer 22 APU coupon surface was dip-coated in the slurry. The coated samples were heat-treated in air at 900°C for 2 h.

2.3. Materials and coating characterizations

In order to identify the crystal structures and phases, X-ray diffraction (XRD) patterns were recorded with an automated Rigaku diffractometer (2500 D/MAX, Rigaku) using Cu K_a radiation. The measurements were conducted over a scanning angle range of 20 - 80° at a scan rate of 5° min^{-1}. The morphological and compositional properties were characterized by scanning electron microscopy (SEM, Hitachi X-4900) coupled with energy dispersive X-ray spectroscopy (EDS, Horiba). The electrical properties, such as the electrical conductivity of the sintered specimen and the area-specific resistance (ASR) of the coated specimen, were measured in air at various temperatures using a DC four-probe technique (Keithley 2400). To provide electrical conduction for the ASR measurement, two separate pairs of Pt probes were attached to both sides of the substrate so that one pair would conduct the current and the other pair would sense the voltage across the thickness. The thermal expansion property of the sintered sample was evaluated from room temperature to 800°C in air using a dilatometer (DIL 402C).

3. Results and Discussion

Given that fine particles exhibit higher sinterability compared with large-scale particle agglomerates, in this study, nano-sized powders of $LaNiO_3$-based perovskites were synthesized to achieve improvement in densification of protective coatings on metallic interconnects. $LaNiO_3$-based perovskites were prepared by the Pechini method, which has been well-known as a useful technique for preparing nano-sized oxide powders. Fig. 1 presents the powder XRD patterns for the synthesized perovskites – $LaNiO_3$ (LNO), $LaNi_{0.6}Co_{0.4}O_3$ (Co–LNO), $LaNi_{0.6}Cu_{0.4}O_3$ (Cu–LNO), and $LaNi_{0.6}Fe_{0.4}O_3$ (Fe–LNO). The powders were obtained after calcination at 800°C. The diffraction peaks for all of the materials can be indexed to the rhombohedral $LaNiO_3$ perovskite phase (JCPDS No. 33-0711).[21] No secondary or impurity phases were detected in the XRD patterns. The splitting of the diffraction peaks (double peaks) at 2θ = 32–33° is attributed to the rhombohedral distortion of the perovskite octahedra.[22] It can be seen in Fig. 1 that the XRD data for the synthesized perovskites display similar profiles, which indicates that the incorporation of Co, Cu, or Fe into $LaNiO_3$ caused no significant change in the perovskite structure. The slight peak shifts observed in the XRD patterns of the doped perovskites (Co–LNO, Cu–LNO, and Fe–LNO) are mainly due to differences in the ionic sizes of Ni and the dopants.[23]

Figure 2(a) - (d) provide SEM images of the Pechini-derived LNO, Co–LNO, Cu–LNO, and Fe–LNO powders, respectively. From the SEM micrographs, it can be seen that the powders were composed of nano-sized particles with sizes of 100–150 nm in soft agglomerates, depending on the dopant incorporated into the structure. The Cu–LNO

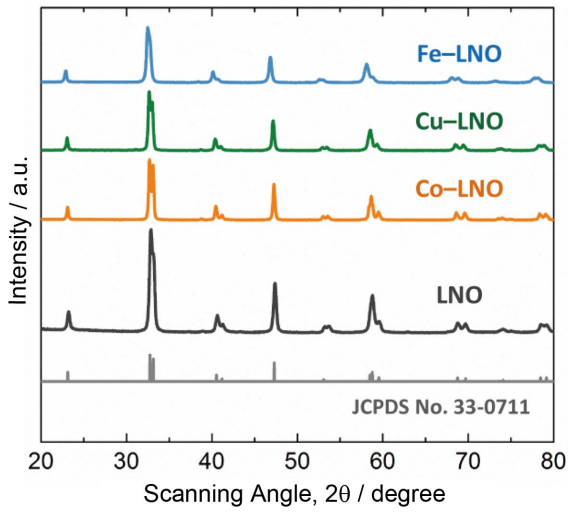

Fig. 1. Powder XRD patterns for LNO, Co–LNO, Cu–LNO, and Fe–LNO synthesized by the Pechini method and calcined at 800°C.

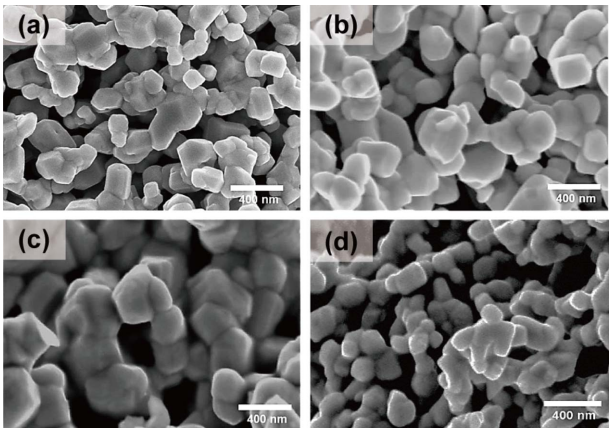

Fig. 2. SEM micrographs of the Pechini-derived perovskite powders: (a) LNO, (b) Co–LNO, (c) Cu–LNO, and (d) Fe–LNO.

powder shows larger particle sizes in comparison to those of the other powders, indicating that Cu doping led to slight particle growth during the calcination process. The nano-sized perovskite particles prepared in this work are expected to exhibit the high sinterability required for the fabrication of protective coatings on metallic interconnects.[24,25] The protective coatings should have high electrical conductivity to reduce ohmic losses and to effectively conduct electrons between the electrodes of the adjacent cells. The Pechini-derived perovskite powders were sintered in air at 1050°C; then, their electrical conducting properties were determined in air at various temperatures ranging from 550 to 850°C. As shown in Fig. 3, the electrical conductivity of the synthesized perovskites decreased gradually with increasing temperature, which indicates metallic conduction behavior, as has been reported in previous studies.[22,26–29] The conductivity values of the doped LNO perovskites were found to be higher than those of pure LNO

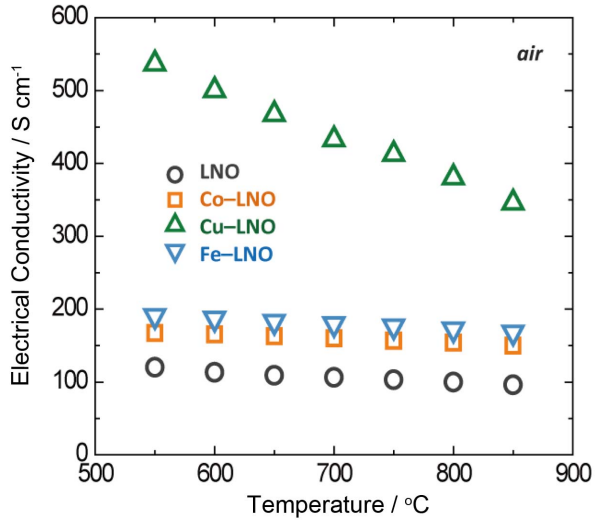

Fig. 3. Plots of electrical conductivity *vs.* temperature for the sintered perovskites measured in air.

over the whole temperature range, proving the beneficial role of dopants in improving the perovskite's electrical properties. In particular, the Cu–LNO perovskite exhibited a conductivity value of 390.5 S cm^{-1} at 800°C, which was much higher than that of LNO (100.6 S cm^{-1}).

The XRD results (data not shown) indicated that LNO and Cu–LNO undergo phase decomposition at 1050°C, while the perovskite structures of Co–LNO and Fe–LNO remain unchanged. In addition to the dopant's role in facilitating electronic conduction, therefore, the high structural stability might be responsible for the improved conductivity observed for Co–LNO and Fe–LNO. Despite its promising conducting property, Cu–LNO has a structural stability problem that is of potential concern for its application as a protective coating. As will be shown later, in fact, Cu–LNO was unable to serve as an efficient coating for SOFC interconnects. Further work is currently being undertaken to study in more detail the stability of the doped LNO perovskites at high temperatures; results will be reported in a subsequent paper.

Another important characteristic of a protective coating is the compatibility of its thermal expansion properties to the metallic interconnect; that is, the coefficient of thermal expansion (CTE) of a coating material must be similar to that of a metallic interconnect. Thermal expansion mismatches between coatings and substrates may cause cracking or delamination due to mechanical stresses that can develop during thermal cycling and/or long-term operation, leading to significant performance degradation. Fig. 4 illustrates the linear expansion *vs.* temperature curves of the perovskite materials, measured during heating from room temperature to 800°C. As shown in Fig. 4, the thermal expansion behaviors exhibit a good linearity with temperature up to 800°C. The average CTE values of LNO, Co–LNO, Cu–LNO, and Fe–LNO were determined to be $16.1 \times 10^{-6}°C^{-1}$, $13.3 \times 10^{-6}°C^{-1}$, $13.5 \times 10^{-6}°C^{-1}$, and $11.4 \times 10^{-6}°C^{-1}$, respectively. These results show that the partial substitution of Co, Cu and Fe for Ni can make the thermal expansion property more compatible with that of the Crofer 22 APU substrate ($12.3 \times 10^{-6}°C^{-1}$).[30]

As a next step, using the Pechini-derived perovskite powders, protective layers were coated on the Crofer 22 APU substrate. A slurry dip-coating process was used; the slurry composition and coating conditions were carefully controlled to reproducibly obtain a thin and uniform layer. To prevent possible damage to the metallic substrate during high-temperature sintering, the coated Crofer samples were heat-treated in air at a relatively low temperature (900°C). SEM images of the surfaces and cross-sections of the perovskite coatings taken after heat-treatment are shown in Fig. 5. Perovskite coatings with thickness values of *ca.* 20 - 22 μm were obtained. Although some pores are visible on the surfaces as well as on the cross-sections of the perovskite coatings, continuous pore networks were only rarely observed across the coating thickness. The surface morphology of the Cu–LNO-coated sample appears to be more porous than

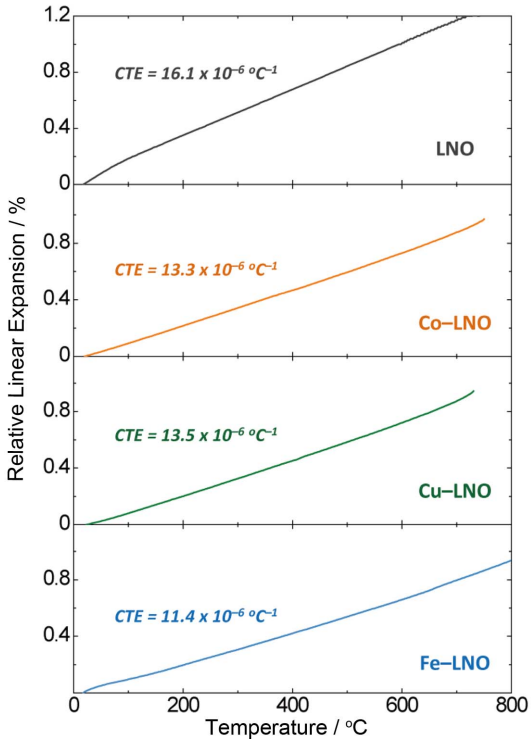

Fig. 4. Plots of relative linear expansion *vs.* temperature for the sintered perovskites measured in air.

those of the other samples, which suggests excessive grain growth of Cu–LNO particles during the heat-treatment process. EDS analysis was also performed on the perovskite-coated interconnects to evaluate the elemental distribution, with results shown in Fig. 5. The EDS results indicate the presence of a chromia layer at the interface between the coating and the substrate, as shown by the sharp increase of Cr concentration. Overall, no significant Cr migration from the interconnect to the protective coating was found to occur during heat-treatment; however, some Cr species were detected in the Cu–LNO coating, indicating that the Cu–LNO coating cannot effectively inhibit the migration of Cr species, probably due to its relatively high porosity, which was revealed by SEM analysis.

Given that Cr species is known to cause cathode poisoning, the perovskite coatings (LNO, Co–LNO, and Fe–LNO) in which no Cr element was observed were selected for the electrical performance test. The ASR value was experimentally measured to evaluate the electrical property of the Crofer interconnects with protective coatings in an air atmosphere. Fig. 6 illustrates the ASR values of the coated Crofer interconnects measured at various temperatures. The samples were oxidized in air at 800°C for 24 h prior to the measurements. The ASR values were reduced by the partial substitution of Co and Fe for Ni, which could be

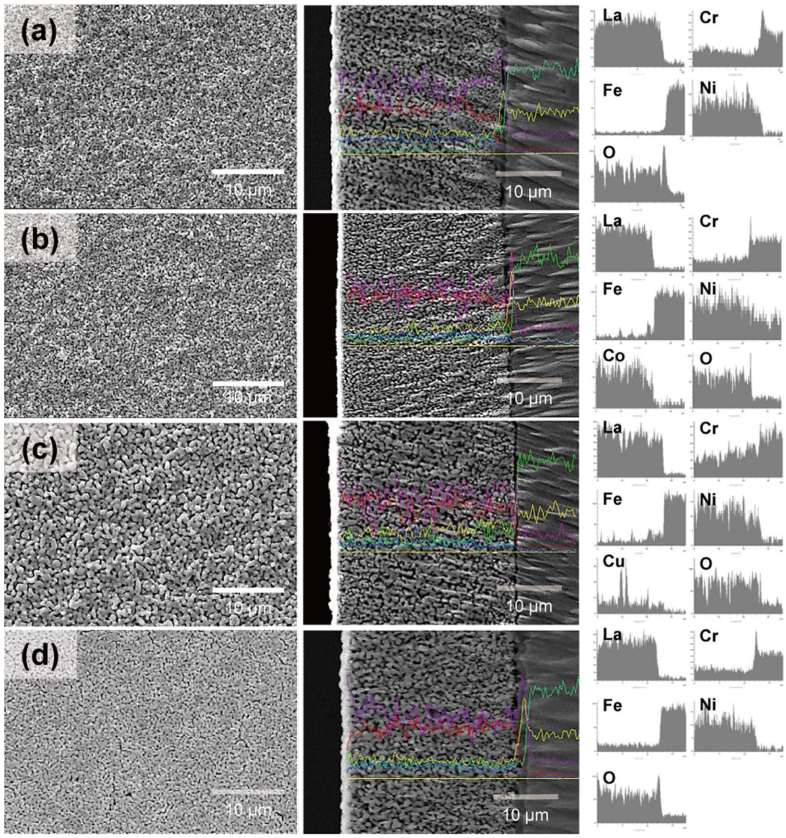

Fig. 5. SEM micrographs of the surface and cross-section of the (a) LNO, (b) Co–LNO, (c) Cu–LNO, and (d) Fe–LNO coatings on the Crofer 22 APU interconnects. The concentration profiles of various elements across the coated interconnects, obtained by EDS analysis are also presented.

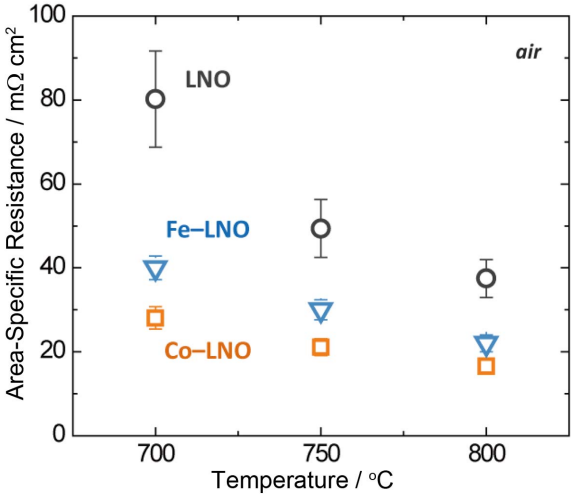

Fig. 6. Area-specific resistances of the Crofer 22 APU interconnects coated with LNO, Co–LNO, and Fe–LNO measured in air at various temperatures.

explained by the higher electrical conductivity (Fig. 3) of the doped LNO perovskites. In particular, the Co–LNO-coated Crofer interconnect exhibited an ASR value as low as 16.5 mΩ cm^2 at 800°C. The results presented here demonstrate that Co–LNO and Fe–LNO coatings are capable of effectively suppressing chromia growth on the metallic interconnects of SOFCs.

4. Conclusions

$LaNiO_3$ (LNO) perovskite oxides doped with Co, Cu, and Fe were synthesized by the Pechini method and were applied as protective coatings on metallic interconnects (Crofer 22 APU). The doped LNO perovskites exhibited improved electrical conductivity and excellent thermal expansion compatibility with the Crofer interconnect. The dense perovskite coatings were fabricated on the Crofer interconnects by a slurry coating process and subsequent heat-treatment. The perovskite-coated interconnects showed ASR values as low as 16.5–37.5 mΩ cm^2 at 800°C, proving the feasibility of using $LaNiO_3$-based perovskites as protective coatings for SOFC interconnects.

Acknowledgments

This work was supported by the Materials Technology Development Program (Phase II) (KEIT Project No. 10051003) and by the New & Renewable Energy Core Technology Program (KETEP Project No. 20143030031440), which were funded by the Ministry of Trade, Industry & Energy, Republic of Korea.

REFERENCES

1. J. P. P. Huijsmans, F. P. van Berkel, and G. M. Christie, "Intermediate Temperature SOFC – a Promise for the 21st Century," *J. Power Sources*, **71** [1-2] 107-10 (1998).
2. W. Z. Zhu and S. C. Deevi, "Development of Interconnect Materials for Solid Oxide Fuel Cells," *Mater. Sci. Eng. A*, **348** [1-2] 227-43 (2003).
3. T. Brylewski, M. Nanko, T. Maruyama, and K. Przybylski, "Application of Fe-16Cr Ferritic Alloy to Interconnector for a Solid Oxide Fuel Cell," *Solid State Ionics*, **143** [2] 131-50 (2001).
4. I. Antepara, I. Villarreal, L. M. Rodríguez-Martínez, N. Lecanda, U. Castro, and A. Laresgoiti, "Evaluation of Ferritic Steels for Use as Interconnects and Porous Metal Supports in IT-SOFCs," *J. Power Sources*, **151** [1-2] 103-7 (2005).
5. J. W. Fergus, "Metallic Interconnects for Solid Oxide Fuel Cells," *Mater. Sci. Eng. A*, **397** [1-2] 271-83 (2005).
6. X. Chen, P. Y. Hou, C. P. Jacobson, S. J. Visco, and L. C. De Jonghe, "Protective Coating on Stainless Steel Interconnect for SOFCs: Oxidation Kinetics and Electrical Properties," *Solid State Ionics*, **176** [5-6] 425-33 (2005).
7. P. Huczkowski, N. Christicmsen, V. Shemet, L. Niewolak, J. Piron-Abellan, L. Singheiser, and W. J. Quadakkers, "Growth Mechanisms and Electrical Conductivity of Oxide Scales on Ferritic Steels Proposed as Interconnect Materials for SOFC's," *Fuel Cells*, **6** [2] 93-9 (2006).
8. Z. Yang, K. S. Weil, D. M. Paxton, and J. W. Stevenson, "Selection and Evaluation of Heat-resistant Alloys for SOFC Interconnect Applications," *J. Electrochem. Soc.*, **150** [9] A1188-201 (2003).
9. S. J. Geng, J. H. Zhu, and Z. G. Lu, "Evaluation of Several Alloys for Solid Oxide Fuel Cell Interconnect Application," *Scr. Mater.*, **55** [3] 239-42 (2006).
10. Y. Matsuzaki and I. Yasuda, "Dependence of SOFC Cathode Degradation by Chromium-containing Alloy on Compositions of Electrodes and Electrolytes," *J. Electrochem. Soc.*, **148** [2] A126-31 (2001).
11. Y. D. Zhen, J. Li, and S. P. Jiang, "Oxygen Reduction on Strontium-Doped $LaMnO_3$ Cathodes in the Absence and Presence of an Iron-chromium Alloy Interconnect," *J. Power Sources*, **162** [2] 1043-52 (2006).
12. S. N. Lee, A. Atkinson, and J. A. Kilner, "Effect of Chromium on $La_{0.6}Sr_{0.4}Co_{0.2}Fe_{0.8}O_3$-Solid Oxide Fuel Cell Cathodes," *J. Electrochem. Soc.*, **160** [6] F629-35 (2013).
13. Z. Yang, G. G. Xia, X. H. Li, and J. W. Stevenson, "$(Mn,Co)_3O_4$ Spinel Coatings on Ferritic Stainless Steels for SOFC Interconnect Applications," *Int. J. Hydrogen Energy*, **32** [16] 3648-54 (2007).
14. W. Qu, L. Jian, J. M. Hill, and D. G. Ivey, "Electrical and Microstructural Characterization of Spinel Phases as Potential Coatings for SOFC Metallic Interconnects," *J. Power Sources*, **153** [1] 114-24 (2006).
15. W. Quadakkers, "Compatibility of Perovskite Contact Layers between Cathode and Metallic Interconnector Plates of SOFCs," *Solid State Ionics*, **91** [1-2] 55-67 (1996).
16. D. P. Lim, D. S. Lim, J. S. Oh, and I. W. Lyo, "Influence of Post-treatments on the Contact Resistance of Plasma-Sprayed $La_{0.8}Sr_{0.2}MnO_3$ Coating on SOFC Metallic Interconnector," *Surf. Coatings Technol.*, **200** [5-6] 1248-51 (2005).
17. J. J. Choi, D. S. Park, B. D. Hahn, J. Ryu, and W. H. Yoon,

"Oxidation Behavior of Ferritic Steel Alloy Coated with Highly Dense Conducting Ceramics by Aerosol Deposition," *J. Am. Ceram. Soc.*, **91** [8] 2601-6 (2008).

18. J. J. Choi, J. Ryu, B. D. Hahn, W. H. Yoon, B. K. Lee, J. H. Choi, and D. S. Park, "Ni-containing Conducting Ceramic as an Oxidation Protective Coating on Metallic Interconnects by Aerosol Deposition," *J. Am. Ceram. Soc.*, **1618** 1614-18 (2010).
19. C. S. Ni, D. F. Zhang, C. Y. Ni, and Z. M. Wang, "Ruddlesden-Popper Nickelate as Coating for Chromia-forming Stainless Steel," *Int. J. Hydrogen Energy*, **39** 13314-19 (2014).
20. W. Z. Zhu and S. C. Deevi, "Opportunity of Metallic Interconnects for Solid Oxide Fuel Cells: A Status on Contact Resistance," *Mater. Res. Bull.*, **38** [6] 957-72 (2003).
21. P. Odier, M. Municken, M. Crespin, F. Dubois, P. Mouron, and J. Choisnet, "Sol-gel Synthesis and Structural Characterisation of the Perovskite Type Pseudo Solid Solution $LaNi_{0.5}Cu_{0.5}O_3$," *J. Mater. Chem.*, **12** [5] 1370-73 (2002).
22. M. Bevilacqua, T. Montini, C. Tavagnacco, G. Vicario, P. Fornasiero, and M. Graziani, "Influence of Synthesis Route on Morphology and Electrical Properties of $LaNi_{0.6}Fe_{0.4}O_3$," *Solid State Ionics*, **177** [33-34] 2957-65 (2006).
23. R. D. Shannon, "Revised Effective Ionic Radii and Systematic Studies of Interatomic Distances in Halides and Chalcogenides," *Acta Cryst.*, **A32** 751-67 (1976).
24. Y. Zhang, A. Javed, M. Zhou, S. Liang, and P. Xiao, "Fabrication of Mn-Co Spinel Coatings on Crofer 22 APU Stainless Steel by Electrophoretic Deposition for Interconnect Applications in Solid Oxide Fuel Cells," *Int. J. Appl. Ceram. Technol.*, **11** [2] 332-41 (2014).
25. B. K. Park, J. W. Lee, S. B. Lee, T. H. Lim, S. J. Park, C. O. Park, and R. H. Song, "Cu- and Ni-Doped $Mn_{1.5}Co_{1.5}O_4$ Spinel Coatings on Metallic Interconnects for Solid Oxide Fuel Cells," *Int. J. Hydrogen Energy*, **38** [27] 12043-50 (2013).
26. R. Chiba, F. Yoshimura, and Y. Sakurai, "An Investigation of $LaNi_{1-x}Fe_xO_3$ as a Cathode Material for Solid Oxide Fuel Cells," *Solid State Ionics*, **124** [3] 281-88 (1999).
27. E. Bucher and W. Sitte, "Defect Chemical Analysis of the Electronic Conductivity of Strontium-substituted Lanthanum Ferrite," *Solid State Ionics*, **173** [1-4] 23-28 (2004).
28. K. Park, J. S. Son, S. I. Woo, K. Shin, M. W. Oh, S. D. Park, and T. Hyeon, "Colloidal Synthesis and Thermoelectric Properties of La-doped $SrTiO_3$ Nanoparticles," *J. Mater. Chem. A*, **2** [12] 4217-24 (2014).
29. J. Y. Tak, S. M. Choi, W. S. Seo, and H. K. Cho, "Thermoelectric Properties of a Doped $LaNiO_3$ Perovskite System Prepared Using a Spark-plasma Sintering Process," *Electron. Mater. Lett.*, **9** [4] 513-16 (2013).
30. Y. Xu, Z. Wen, S. Wang, and T. Wen, "Cu Doped Mn-Co Spinel Protective Coating on Ferritic Stainless Steels for SOFC Interconnect Applications," *Solid State Ionics*, **192** [1] 561-64 (2011).